

Does the configurational entropy of polydisperse particles exist?

Misaki Ozawa¹ and Ludovic Berthier¹

Laboratoire Charles Coulomb, UMR 5221 CNRS-Université de Montpellier, Montpellier, France

Classical particle systems characterized by continuous size polydispersity, such as colloidal materials, are not straightforwardly described using statistical mechanics, since fundamental issues may arise from particle distinguishability. Because the mixing entropy in such systems is divergent in the thermodynamic limit we show that the configurational entropy estimated from standard computational approaches to characterize glassy states also diverges. This reasoning would suggest that polydisperse materials cannot undergo a glass transition, in contradiction to experiments. We explain that this argument stems from the confusion between configurations in phase space and states defined by free energy minima, and propose a simple method to compute a finite and physically meaningful configurational entropy in continuously polydisperse systems. Physically, the proposed approach relies on an effective description of the system as an M^* -component system with a finite M^* , for which finite mixing and configurational entropies are obtained. We show how to directly determine M^* from computer simulations in a range of glass-forming models with different size polydispersities, characterized by hard and soft interparticle interactions, and by additive and non-additive interactions. Our approach provides consistent results in all cases and demonstrates that the configurational entropy of polydisperse system exists, is finite, and can be quantitatively estimated.

I. CONFIGURATIONAL ENTROPY IN POLYDISPERSE SYSTEMS

Colloidal systems play an important role in a wide spectrum of soft condensed matter physics, from crystallization kinetics to the glass transition phenomenon. An important motivation is that colloids can be seen as “big atoms”, which may prove useful in terms of microscopic observations and particle design¹. These colloidal particles are composed of a very large number of atoms, such that each colloid in a given experimental batch is a unique object. Therefore, colloidal particles are distinguishable classical objects, which rises subtle theoretical issues for their statistical mechanical treatment². In particular, colloidal particles are often characterized by a continuous distribution $f(\sigma)$ of particle diameters, σ . Thus, in principle, colloids can be readily distinguished by their sizes and there are no two identical particles in the system. Polydisperse systems are widely employed in studies of the glass transition because polydispersity efficiently prevents crystallization. Therefore, understanding how polydispersity impacts the theoretical treatment of glass formation is an important question that constitutes the main theme of this paper.

The statistical mechanics of continuously polydisperse systems has been widely studied in a number of contexts^{3–7}. Particle distinguishability may cause in particular some subtle issues, such as the well-known Gibbs paradox⁸ and this requires special attention². In that case, particle indistinguishability stemming from a quantum mechanical treatment cannot be invoked for colloidal particles⁹.

Before proceeding to our discussion of disordered materials, let us recall what happens in the case of ordered materials. In a recent article, Cates and Manoharan discuss the existence of a colloidal crystal made of weakly polydisperse hard spheres²: “In the fluid, the spheres can easily swap places whereas in the crystal, they cannot.

For indistinguishable particles, the entropy gain on transforming from liquid to crystal is extensive. The additional entropy cost of localizing distinguishable particles onto un-swappable lattice sites contains a term $k_B \ln(N!)$ where $N!$ counts particle permutations. This term must be paid to collapse an accessible phase-space volume in which distinguishable particles can change places, into one where they cannot. This putative entropy cost is supra-extensive ($k_B N \ln N$) and thus for large N outweighs the extensive entropy on formation of the crystal. Thus the kinetic approach to entropy predicts that colloidal crystals are thermodynamically impossible. Yet they are observed every day.” This paradox is resolved by including the $N!$ distinct crystal *configurations* generated by the permutation of N distinguishable particles in a single crystalline *state*. Then, this $N!$ multiplicity term cancels exactly the putative entropy cost due to particle distinguishability². Physically, this theoretical treatment corresponds to describing the polydisperse system as behaving effectively as a one-component system and it highlights the conceptual difference between *configurations* in phase space volume and *states* defined from free energy minima, which are usually constructed from a much larger number of configurations. These basic ideas will reappear throughout our discussion of disordered materials.

Another well-known issue arising in continuously polydisperse systems is the divergence of the mixing entropy, S_{mix} ^{3,9,10}. Mathematically, this is because the mixing entropy of a discrete mixture of particles diverges in the limit of an infinite number of components, which is needed to formally represent a continuous distribution in the thermodynamic limit. In several situations, this divergent contribution is immaterial, for instance when discussing phase equilibria with a fixed particle size distribution $f(\sigma)$ ⁷ or mixing processes of two different continuous polydisperse systems¹¹, because the absolute value of the entropy is irrelevant and only entropy differences between

two systems matter^{7,9,11}. In the above-mentioned cases, the diverging contributions to S_{mix} cancel each other.

All these issues are relevant for a proper treatment of the glass transition in polydisperse materials, but this has never been carefully discussed before. The configurational entropy S_{conf} is the central quantity to describe the thermodynamics of supercooled liquids approaching the glass transition^{12–14}. Conventionally in computer simulations (and also in experiments), S_{conf} is defined as $S_{\text{conf}} = S_{\text{tot}} - S_{\text{vib}}$, where S_{tot} is the total entropy of the system and S_{vib} is the entropy of the glass (or vibrational) state where only particle vibrations due to thermal fluctuations take place^{12–14}. Physically, S_{conf} quantifies the number of available amorphous states in glassy systems. These metastable states are understood as long-lived free energy minima¹⁴, even though their mathematical definition in finite dimensional glass models remains problematic¹⁵. The mean-field theory of the glass transition is based on the existence of an ideal glass transition occurring at temperature T_K at which S_{conf} vanishes¹⁶. Hence, there is a need for a careful investigation of the entropy of polydisperse glassy materials.

An extension of the argument developed by Cates and Manoharan for the polydisperse crystal² can be made for the configurational and mixing entropies of a polydisperse glass. In that case, the system transforms from the fluid where particle swaps are easy to the glass where they are not. In multi-component glass-formers, the entropy of the fluid state must contain a mixing entropy contribution S_{mix} , because the particles can exchange their positions^{17–20}. It is conventionally assumed that S_{vib} does not contain the mixing contribution²¹, because particles in the glass state mainly vibrate around a fixed averaged position in a given glass configuration and particle exchanges are neglected. Pushing further this argument, the divergence of S_{mix} for continuous polydispersity provokes the divergence of the entropy of the fluid, whereas the glass entropy remains finite. Logically, then, if the configurational entropy is infinite in the fluid, it cannot vanish and the glass transition cannot exist. This reasoning is of course in direct contradiction with experiments and simulations, where “polydisperse glasses are observed every day”, to paraphrase Cates and Manoharan.

The goal of this paper is to provide a conceptually-correct and computationally-simple way to define and measure the configurational entropy in continuously polydisperse systems. There exist many separate studies of the glassy behavior of colloidal and polydisperse systems both in experiments^{22,23} and simulations^{24–28} and of the configurational entropy in glass-forming models^{18,20,29–37}. However, we are not aware of any detailed theoretical or numerical treatment of the configurational entropy for continuously polydisperse systems, for which standard methods are not valid, as we just showed. Our paper thus fills this gap.

Our basic idea is to treat a continuously polydisperse system as an effective M^* -component system with a *finite*

number of components M^* , which can take real values. Within this approach, the glass entropy then also contains a diverging contribution which cancels the one in the total entropy S_{tot} . In other words, we estimate a finite and physically-relevant contribution to the mixing entropy, which we call an effective mixing entropy S_{mix}^* . As a result, we obtain a finite estimate for the configurational entropy S_{conf} as well. This treatment thus shows that the configurational entropy of polydisperse systems is always finite, and may possibly vanish at a glass transition. In addition, we propose a numerical method to determine M^* and S_{mix}^* , which is generically applicable to any glass-forming computer model.

Before closing this introduction, we need to mention that recently, an alternative method to compute the configurational entropy was proposed³¹, which is based on the Franz-Parisi construction³⁸. In this approach, the configurational entropy is estimated as a free energy difference, and it is measured in monodisperse and polydisperse systems in the exact same way. Thus, this method automatically produces finite values of the configurational entropy without suffering from a divergent mixing entropy, and the problems mentioned above are automatically bypassed. Results using this method for a continuous polydisperse system have only very recently been obtained³⁹. Because this approach is numerically more demanding than the standard ones discussed in this paper, it is useful to make the latter applicable to polydisperse systems, such that both types of methods can be compared.

The paper is organized as follows. In Sec. II, we propose our theoretical idea to compute the configurational entropy in continuous polydisperse system. In Sec. III, we describe the numerical method to determine M^* and S_{mix}^* . In Sec. IV, we validate our approach for several simulation models. In Sec. V, we provide a discussion of our results together with some perspectives.

II. THEORETICAL CONSIDERATIONS: THE MAIN PROBLEM AND ITS PHYSICAL RESOLUTION

In this section, we present our approach to compute the configurational entropy in continuously polydisperse systems. We first fix the notations and give some definitions. We then introduce a simple theoretical model of a binary mixture illustrating the core problem to be faced. Through the discussion and resolution of the paradoxical results obtained in this simple model, we draw more general conclusions which lead to our simple proposal to analyze the configurational entropy of generic polydisperse systems.

A. Mixing entropy in polydisperse systems

We first provide definitions and notations related to the statistical mechanics and mixing entropy in mixtures

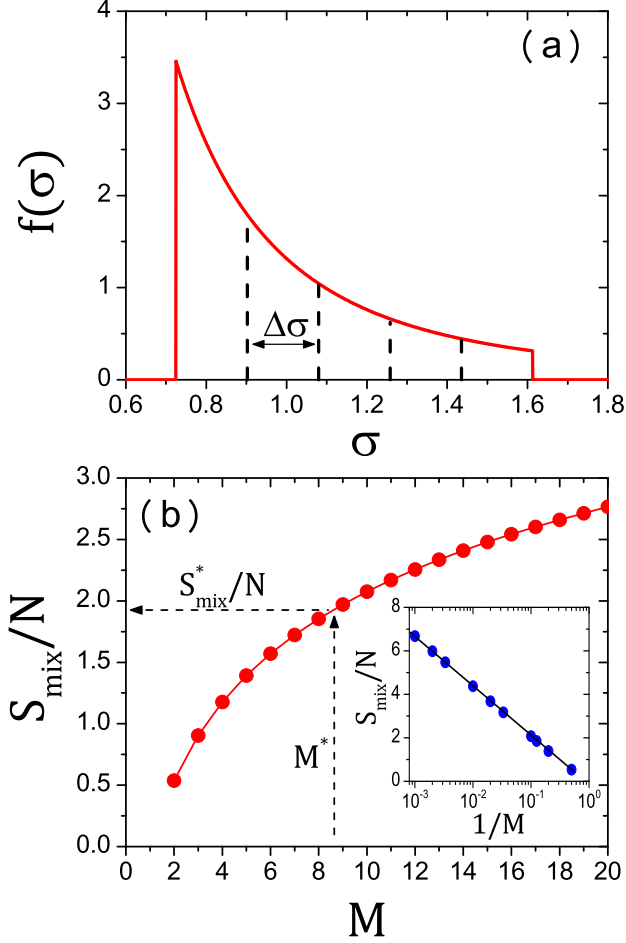


FIG. 1. (a) Particle size distribution $f(\sigma) = A\sigma^{-3}$ for $\sigma \in [\sigma_{\min}, \sigma_{\max}]$, $f(\sigma) = 0$ outside this range. The dashed lines illustrate the decomposition of $f(\sigma)$ into the arbitrary example of $M = 5$ species, with $\Delta\sigma = (\sigma_{\max} - \sigma_{\min})/M$. (b) The mixing entropy S_{mix} computed from Eqs. (5, 8). The dashed arrows define the value of S_{mix}^* from an effective value M^* . The inset demonstrates the logarithmic divergence of S_{mix}/N when $M \rightarrow \infty$.

of particles. We consider a continuously polydisperse system whose particle size distribution is given by $f(\sigma)$. To derive the mixing entropy of this system, we decompose $f(\sigma)$ into an integer number M of species^{3,9,10}, as illustrated in Fig. 1(a) for a specific example. The continuously polydisperse system is recovered in the limit $M \rightarrow \infty$.

We consider the canonical ensemble characterized by the number of particles N , the volume V , and the temperature $T = 1/\beta$. We set the Boltzmann constant to unity. The partition function Z_{tot} of the system is

$$Z_{\text{tot}} = \frac{1}{\Pi_{m=1}^M N_m! \Lambda^{dN}} \int_V d\mathbf{r}^N e^{-\beta U(\mathbf{r}^N)}, \quad (1)$$

where Λ , d , and U are the de Broglie thermal wavelength, spatial dimension, and potential energy, respec-

tively. For simplicity, we consider equal masses (hence equal Λ) irrespective of species throughout this paper. N_m is the number of particles within species m , such that $N = \sum_{m=1}^M N_m$. Note that the term, $1/\Pi_{m=1}^M N_m!$ (or more simply $1/N!$ when $m = 1$), should be included irrespective of distinguishability of the particles in order to obtain an extensive free energy^{2,5,8,9} (see also recent numerical verifications in Refs. 32 and 33). The total free energy of the system is

$$\beta F_{\text{tot}} = -\ln Z_{\text{tot}}. \quad (2)$$

Then, the total entropy S_{tot} can be written as

$$S_{\text{tot}} = \beta(E_{\text{tot}} - F_{\text{tot}}) \sim \ln Z_{\text{tot}} \sim -\ln(\Pi_{m=1}^M N_m!), \quad (3)$$

where E_{tot} is the total energy of the system. In this paper, we use the symbol “ \sim ” to single out the contribution due to the mixing entropy. Instead, we use the symbol “ \simeq ” to express the conventional “nearly equal” relation. By applying Stirling’s approximation, $\ln x! \simeq x \ln x - x$ ($x \gg 1$), we get

$$\ln(\Pi_{m=1}^M N_m!) \simeq (N \ln N - N) + N \sum_{m=1}^M X_m \ln X_m, \quad (4)$$

where $X_m = N_m/N$ is the concentration of species m . The second term in Eq. (4) comes from the effect of having a system with M components, *i.e.*, from the size polydispersity. The mixing entropy $S_{\text{mix}}^{(M)}$ is defined as

$$S_{\text{mix}}^{(M)} = -N \sum_{m=1}^M X_m \ln X_m. \quad (5)$$

For latter purposes, we note that the mixing entropy provides a contribution to the total entropy S_{tot} . Using the ‘ \sim ’ notation introduced above, we have

$$S_{\text{tot}} \sim S_{\text{mix}}^{(M)}. \quad (6)$$

We can clearly see that in a continuously polydisperse case, when we have $M = N$ and hence $X_m = 1/N$, the mixing entropy $S_{\text{mix}}^{(M)}$ diverges in the thermodynamic limit, $N \rightarrow \infty$,

$$\frac{S_{\text{mix}}^{(M=N)}}{N} = -\sum_{m=1}^N \frac{1}{N} \ln \frac{1}{N} = \ln N \xrightarrow{N \rightarrow \infty} \infty. \quad (7)$$

Alternatively, if we represent a system characterized by a continuous size distribution $f(\sigma)$ as an M -component mixture, then we divide the distribution into M equal intervals, $\Delta\sigma = (\sigma_{\max} - \sigma_{\min})/M$, see Fig. 1(a) for an example. Therefore we have

$$X_m = \int_{\sigma_m}^{\sigma_{m+1}} d\sigma f(\sigma), \quad (8)$$

where $\sigma_m = \sigma_{\min} + (m-1)\Delta\sigma$. Using Eqs. (5) and (8), we get S_{mix} as a function of M . In Fig. 1(b), we show

$S_{\text{mix}}^{(M)}$ for a specific example of $f(\sigma)$ which will be studied numerically below. In the inset of Fig. 1(b), we confirm that S_{mix}/N diverges logarithmically in the continuous polydisperse limit, $M \rightarrow \infty$ (or $\Delta\sigma \rightarrow 0$)^{3,9,10}, as expected.

Note that in Refs. 3, 9, and 10, a formal expression of the continuous polydisperse limit is given by

$$\begin{aligned} \lim_{M \rightarrow \infty} \frac{S_{\text{mix}}^{(M)}}{N} &= - \lim_{\substack{M \rightarrow \infty \\ \Delta\sigma \rightarrow 0}} \sum_{m=1}^M f(\sigma_m) \Delta\sigma \ln(f(\sigma_m) \Delta\sigma) \\ &= - \int_0^\infty d\sigma f(\sigma) \ln f(\sigma) - \lim_{\Delta\sigma \rightarrow 0} \ln \Delta\sigma. \end{aligned} \quad (9)$$

In this expression, the divergent mixing entropy is decomposed into a finite term depending on $f(\sigma)$ (the first term) and a divergent term (the second term) in Eq. (9). However, the first term is not a well-defined quantity, since it depends on the argument or labeling of the distribution f ¹⁰, and hence one cannot use the first term alone for a physically relevant mixing entropy to compute the configurational entropy.

B. A paradox for binary mixtures

We introduce a simple model of a glass-forming binary mixture whose analysis produces paradoxical results that illustrate the core of the problem that we face regarding the mixing entropy of polydisperse particles. The physics of this system has been discussed qualitatively in Ref. 17.

We consider a binary mixture ($M = 2$) composed of species 1 and 2 in arbitrary dimensions. The diameters of the particles are respectively $\sigma_1 = \sigma$ and $\sigma_2 = \sigma(1 + \epsilon)$, with $\epsilon > 0$. For simplicity, we consider equal concentrations, $X_1 = X_2 = 1/2$. In this setting, the total entropy S_{tot} always contains the mixing entropy S_{mix} irrespective of the absolute value of ϵ , so that the mixing contribution to the total entropy reads

$$S_{\text{tot}} \sim S_{\text{mix}} = N \ln 2. \quad (10)$$

In previous studies of binary mixtures with $\epsilon \simeq 1$, this mixing entropy term was included to compute the configurational entropy and to detect the ideal glass transition^{17–20,40,41}. However, the fact that the mixing entropy does not depend on ϵ is quite surprising. Indeed, when $\epsilon \ll 1$, one can expect that the physics of such a nearly monodisperse system should not be very different from that of purely one-component system obtained by setting $\epsilon = 0$. In particular, the ideal glass transition temperature T_K (or density ϕ_K for hard spheres) of this binary system, if it exists, should not be very different from that of the purely one-component system. More precisely, one would expect that T_K is a continuous function of ϵ near $\epsilon = 0$. However, the configurational entropy S_{conf}/N of the binary system is larger than that of the purely one-component system by $\ln 2 \simeq 0.7$, due to the mixing entropy contribution in Eq. (10), and this large

entropy appears discontinuously as soon as $\epsilon > 0$. The theoretical analysis of this system is therefore physically inconsistent.

One possible solution to the paradox would be to always neglect the mixing entropy contribution, as done for instance in Ref. 42. However, such treatment would change the location of the ideal glass transition significantly. Let us consider two examples to illustrate this point. In the Kob-Andersen (KA) model⁴³, the mixing entropy contributes $S_{\text{mix}}/N \simeq 0.5$ to the total entropy S_{tot} ¹⁸. If one neglects S_{mix}/N from S_{conf}/N , the estimated $T_K \simeq 0.3$ ^{18,19,41} increases to $T_K \simeq 0.5$, a temperature that is actually easily equilibrated in the simulations⁴³. In the binary hard sphere model studied in Ref. 20, one has $S_{\text{mix}}/N = \ln 2 \simeq 0.693$ ²⁰. If one again removes S_{mix}/N , the estimated ideal glass transition density, $\phi_K \simeq 0.62$ ²⁰, is now reduced to $\phi_K \simeq 0.58$, where equilibrium is again easily achieved²⁰. Assuming that the other contributions to the numerical estimate of S_{conf} are well-controlled, then it appears impossible to neglect the mixing entropy.

These examples demonstrate that the mixing entropy term is actually needed for a proper estimate of the configurational entropy. But if so, then it must be included in any binary mixture, including one where $\epsilon \ll 1$. But in that case the limit $\epsilon \rightarrow 0$ produces a jump in the estimated location of the glass transition, which is unphysical.

In summary, when considering our simple example of a binary mixture with size ratio $(1 + \epsilon)$, taking ϵ as a continuous parameter suggests that previous approaches to determine the configurational entropy cannot be applied directly, as one needs to decide *a priori* whether or not to include the mixing entropy in the configurational entropy. Such decision can still produce meaningful results when ϵ is a constant which is either large enough or very small. But when intermediate ϵ values are considered, or when the particle size distribution becomes more complex, an *ad hoc* approach becomes impossible. Importantly for the present work, this approach breaks down completely when the polydispersity becomes continuous, because then a continuous spectrum of large and small ϵ values coexists in a single system.

C. Physical resolution of the binary mixture paradox

To resolve the above paradox, we carefully discuss the vibrational (or glass) state and its entropy. We suppose that the equilibrium system is sufficiently deeply supercooled that there is a strong separation of timescales between vibrations and structural relaxation. This implies that it makes sense to consider a vibrational state.

To compute the vibrational entropy S_{vib} , one must evaluate the partition function of this vibrational state, Z_{vib} , by performing a configurational integral within the restricted phase space volume V_{basin} explored by the system over the vibrational timescale. To perform the con-

figurational integral, a representative basin, denoted by α , is randomly selected and then the configurational integral is evaluated numerically using methods such as the harmonic approximation around the local minimum of the potential energy^{18,19}, or a Frenkel-Ladd⁴⁴ thermodynamic integration over a system constrained by harmonic springs^{17,19,20}.

However, there is a factorial degeneracy of α in the phase space volume. In particular, these basins can be generated by permutation of the particles². Thus, we have to take into account the number of physically identical basins to evaluate Z_{vib} . When $\epsilon \simeq 1$ (corresponding to typical binary mixtures^{18,20}), the multiplicity is simply given by the number of configurations obtained by permuting particles within each species ($1 \leftrightarrow 1$ or $2 \leftrightarrow 2$), and this corresponds to $N_1!N_2!$. Instead, when $\epsilon \ll 1$, the permutation of particles between unlike species ($1 \leftrightarrow 2$) should also be taken into account, because this manipulation also generates configurations belonging to the physically identical basin.

Thus, we need to multiply the configurational integral by $N!$ instead of $N_1!N_2!$. As a result, Z_{vib} is different in the two cases, $\epsilon \simeq 1$ and $\epsilon \ll 1$, as follows,

$$Z_{\text{vib}} = \begin{cases} \frac{N_1!N_2!}{N_1!N_2!\Lambda^{dN}} \int_{V_{\text{basin}}} d\mathbf{r}^N e^{-\beta U(\mathbf{r}^N)} & (\epsilon \simeq 1), \\ \frac{N!}{N_1!N_2!\Lambda^{dN}} \int_{V_{\text{basin}}} d\mathbf{r}^N e^{-\beta U(\mathbf{r}^N)} & (\epsilon \ll 1). \end{cases} \quad (11)$$

Therefore, the vibrational entropy contains a mixing entropy contribution whose value depends explicitly on the value of ϵ ,

$$S_{\text{vib}} \sim \ln Z_{\text{vib}} \sim \begin{cases} 0 & (\epsilon \simeq 1) \\ N \ln 2 & (\epsilon \ll 1). \end{cases} \quad (12)$$

When $\epsilon \simeq 1$, the vibrational entropy does not contain a finite mixing entropy, which is consistent with previous studies^{18,20}. However, when $\epsilon \ll 1$, the vibrational entropy contains a mixing entropy contribution, which originates from the fact that particles with similar (but distinct) sizes can be permuted within the vibrational state. By combining Eqs. (10, 12), we obtain S_{conf} as,

$$S_{\text{conf}} = S_{\text{tot}} - S_{\text{vib}} \sim \begin{cases} N \ln 2 & (\epsilon \simeq 1) \\ 0 & (\epsilon \ll 1). \end{cases} \quad (13)$$

In this reasoning, the mixing entropy contribution to S_{vib} for $\epsilon \ll 1$ exactly cancels the one in S_{tot} and thus S_{conf} does not contain any mixing entropy, which is consistent with the physics of a purely one-component system. As a result, T_K would not change discontinuously between $\epsilon \ll 1$ and the purely one-component system with $\epsilon = 0$, thus resolving the paradox.

What do we learn from this very simple example? First, a binary system can be described by either an effective one-component system or by a truly binary system, depending on the value of ϵ . In practice, these two

cases should be distinguished by investigating the effect of physically swapping the position of particles belonging to different species ($1 \leftrightarrow 2$). One can equivalently consider that the positions of the particles are fixed, while that their diameters are swapped, assuming that the mass of each species is identical. These two views are of course identical, but swapping diameters is more convenient to describe the response of the system to such swaps. From such an analysis, one should be able to determine a critical value ϵ^* of ϵ such that mixtures with diameter ratio characterized by $\epsilon < \epsilon^*$ should be treated as one-component systems, whereas for $\epsilon > \epsilon^*$ a binary description would be needed. Evaluating ϵ^* from a first-principle analysis is a worthwhile goal.

To determine which case is appropriate to describe a given binary mixture, one should determine whether the system remains within the same original basin after swapping the particle diameters between different species. If it does, then an effective one-component description is appropriate, otherwise a binary description is needed. In both cases, S_{vib} and S_{conf} contain a mixing entropy contribution, but its precise value depends on which effective description is selected by the above procedure. Therefore, the general conclusion is that one must always include S_{mix} into S_{vib} , but its value must be numerically determined by a careful analysis of the robustness of the basin to particle diameter swaps.

D. General strategy: Mapping to an effective M^* -component system

Our main idea is that a continuously polydisperse system should be regarded as an effective M^* -component system with $M^* < \infty$. Such a simple idea has been used before for instance to study phase equilibria (see Ref. 7 and references therein) and prediction of the equation of state^{45,46}. In the following, we show how to apply this idea to obtain a meaningful definition of the configurational entropy.

We consider a generic polydisperse system in a sufficiently deeply supercooled liquid regime, where the vibrational entropy can be well-defined. The particle size distribution is characterized by M species, where $M = \infty$ if the polydispersity is continuous.

The physical idea that particles with diameter ratio smaller than a threshold (which we called $(1 + \epsilon^*)$ in the above example of a binary mixture) should be treated as identical suggests that a continuous particle size distribution could be “coarse-grained” into finite bins to be effectively treated as an M^* -component mixture. The value of M^* should be determined by requesting that (i) particle diameter swaps within a single effective species ($m \leftrightarrow m$) leave the basin unaffected (ii) particle diameter swaps between different species ($m \leftrightarrow n$ with $m \neq n$) drive the system out of the original basin.

Once the value of M^* is estimated, then we evaluate the partition function within the vibrational state, Z_{vib} ,

by taking into account the multiplicity of physically identical basins, $\Pi_{m=1}^{M^*} N_m!$, such that

$$Z_{\text{vib}} = \frac{\Pi_{m=1}^{M^*} N_m!}{\Pi_{m=1}^M N_m! \Lambda^{dN}} \int_{V_{\text{basin}}} d\mathbf{r}^N e^{-\beta U(\mathbf{r}^N)}. \quad (14)$$

Note that we use M and M^* in this expression, which respectively represent the actual and effective numbers of components in the polydisperse system.

Using Eqs. (4, 5), the vibrational entropy S_{vib} is then given by

$$S_{\text{vib}} \sim \ln Z_{\text{vib}} \sim S_{\text{mix}}^{(M)} - S_{\text{mix}}^{(M^*)}. \quad (15)$$

Note that S_{vib} contains two mixing entropy terms, the possibly divergent term, $S_{\text{mix}}^{(M)}$, and the finite contribution $S_{\text{mix}}^{(M^*)}$.

Finally, by combining Eq. (15) with the total entropy S_{tot} in Eq. (6), we obtain the configurational entropy S_{conf} ,

$$S_{\text{conf}} = S_{\text{tot}} - S_{\text{vib}} \sim S_{\text{mix}}^{(M^*)}. \quad (16)$$

The remarkable result is of course that the term $S_{\text{mix}}^{(M)}$ which diverges for continuous polydispersity has disappeared from this final result, in which only the finite value $S_{\text{mix}}^{(M^*)}$ remains. We call effective mixing entropy $S_{\text{mix}}^* = S_{\text{mix}}^{(M^*)}$ this physically relevant contribution to the configurational entropy.

It is clear from Eq. (16) that the argument against the existence of an ideal glass transition for continuous polydispersity is now avoided because S_{conf} is always finite and should contain a finite contribution stemming from an effective mixing entropy. Also, the above reasoning demonstrates that the configurational entropy should be interpreted or quantified as the (logarithm of the) number of *states*, and not of *configurations*. In the inherent structure approach⁴⁷ one would count the (infinite) number of configurations (or their corresponding inherent structures) generated by the mixing effect, which would thus result in a diverging configurational entropy⁴⁸. Instead here, each vibrational ‘state’ accounts for an infinite number of configurations (and thus of inherent structures).

In addition, our theoretical strategy provides useful guidelines for estimating numerically the effective mixing entropy S_{mix}^* for any generic polydisperse glass-forming material. In our approach, M^* and thus S_{mix}^* are not arbitrary choices, but they should be determined by the system itself through the response of the basins to diameter swaps. We now describe how to implement these ideas in practice.

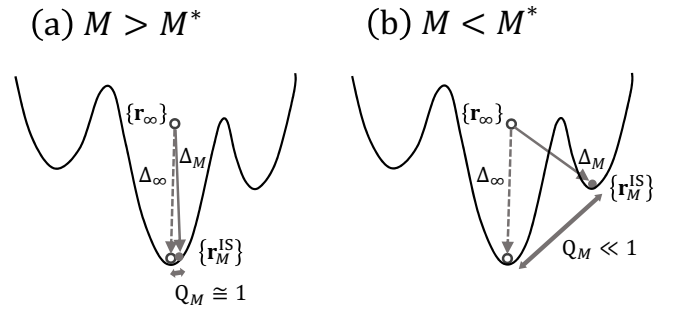


FIG. 2. Sketch of the potential energy landscape showing the initial equilibrium configuration $\{\mathbf{r}_\infty\}$, and the inherent structure $\{\mathbf{r}_M^{\text{IS}}\}$ obtained after swapping the diameters within each M species. (a) When $M > M^*$, the system stays in the same basin so that $Q_M \simeq 1$ and $\Delta_M \simeq \Delta_\infty$. (b) When $M < M^*$, the system moves to another basin so that $Q_M \ll 1$ and $\Delta_M \gg \Delta_\infty$. M^* is defined from the crossover between situations (a) and (b).

III. NUMERICAL IMPLEMENTATION

A. General algorithm for the numerical determination of M^*

As explained in Sec. II, M^* should be such that (i) particle diameter swaps within a single effective species ($m \leftrightarrow m$) leave the basin unaffected (ii) particle diameter swaps between different species ($m \leftrightarrow n$ with $m \neq n$) drive the system out of the original basin.

To determine M^* , we prepare equilibrium configurations of the original continuously polydisperse system characterized by a distribution $f(\sigma)$. We denote by $\{\mathbf{r}_\infty\}$ the original configuration, see Fig. 2. In order to characterize whether the system stays physically in the same basin or moves to another basin as a result of the swaps, we perform a quench of the system into the inherent structure (IS)⁴⁷. The IS corresponding to the initial configuration is denoted as $\{\mathbf{r}_\infty^{\text{IS}}\}$.

We then decompose $f(\sigma)$ into M species, from $M = 1$ where the system is treated as an one-species system, to $M = \infty$ which describes the original system. In practice we stop at the large value $M = 100$. For a given M value, we systematically perform diameter swaps within each species ($m \leftrightarrow m$, with $m = 1, \dots, M$). More precisely, for a given configuration, we randomly pick a pair of particles within the same species and exchange their diameters. We repeat such diameter swap N times so that most of the particles in the configuration experience the swap. Once the swaps have been performed, we quench the obtained configuration to its IS, which we denote by $\{\mathbf{r}_M^{\text{IS}}\}$. Our goal is to monitor whether the system lands in a different basin (for $M < M^*$) or not (for $M > M^*$), as sketched in Fig. 2. To this end we monitor the following three quantities.

- The IS energy $e_{\text{IS}}^{\text{47}}$. When the system moves to another basin, e_{IS} should change from the value it

has in the original basin.

- The overlap Q_M between the IS configurations $\{\mathbf{r}_\infty^{\text{IS}}\}$ and $\{\mathbf{r}_M^{\text{IS}}\}$:

$$Q_M = \frac{1}{N} \sum_{i,j} \theta(a - |\mathbf{r}_{Mi}^{\text{IS}} - \mathbf{r}_{\infty j}^{\text{IS}}|), \quad (17)$$

where $\theta(x)$ is the Heaviside step function, and a is a microscopic threshold lengthscale. By definition, $Q_\infty = 1$, whereas we expect that Q_M decreases from 1 with decreasing M .

- The mean-squared displacement between the original equilibrium configuration $\{\mathbf{r}_\infty\}$ and the swapped IS $\{\mathbf{r}_M^{\text{IS}}\}$:

$$\Delta_M = \frac{1}{N} \sum_{i=1}^N |\mathbf{r}_{Mi}^{\text{IS}} - \mathbf{r}_{\infty i}|^2, \quad (18)$$

so that Δ_∞ corresponds approximately to the plateau value of the mean-squared displacement reached in the physical dynamics of the original system.

If the system falls into a different basin, one expects that Q_M will strongly decay from 1 and that Δ_M will increase significantly from Δ_∞ , as shown in Fig. 2. When $M > M^*$, the system remains in the same basin after the swaps and the quench, showing that $Q_M \simeq 1$ and $\Delta_M \simeq \Delta_\infty$. On the other hand, when $M < M^*$, the original basin is destroyed, and the system moves to another basin, showing that $Q_M \ll 1$ and $\Delta_M \gg \Delta_\infty$. We expect that M^* can be defined as a crossover value between these two extreme cases.

More precisely, we perform the following algorithm to determine M^* .

General Algorithm: Swap and quench protocol

- 1) Define M species by dividing the distribution $f(\sigma)$ into M finite bins.
- 2) Prepare an equilibrium configuration of the original continuous polydisperse system, $\{\mathbf{r}_\infty\}$.
- 3) Randomly pick up a pair of particles within the same bin, and exchange their diameters. Do N such exchanges.
- 4) Quench the system and obtain $\{\mathbf{r}_M^{\text{IS}}\}$.
- 5) Repeat 1) - 4) for a large number of configurations for a wide range of M values, between $M = 1$ and $M = 100$.
- 6) Plot e_{IS} , Q_M and Δ_M as a function of M and determine M^* as a crossover value.

This “swap and quench” protocol is a natural way to determine M^* which follows from the theoretical idea described in Sec. II. In this protocol, the distribution of the particle diameters $f(\sigma)$ is unaffected after defining M and after the diameter swaps.

We have considered the following alternative scheme where one literally performs a discretization of the diameters into M species and monitor the effect of this coarse-graining on the basin. However, we found that this coarse-graining process may affect the thermodynamic state point of the system for soft potentials. Therefore, we use this method only for hard sphere systems so that the volume fraction (and therefore the thermodynamic state point) does not change. For completeness we also present this alternative “coarse-graining and quench” protocol. Most of this procedure is as in the above “swap and quench” protocol except for item 3) which is replaced by:

- 3') Discretize the diameters of the original system into M discrete species keeping the global volume fraction constant.

We have checked that the two protocols give essentially the same results for hard spheres, as shown below. We mention the coarse-graining procedure as a way to trigger the imagination of future researchers towards the implementation of numerical procedures alternative to ours.

B. Details of our models and simulations

We perform molecular simulations for several pair potentials in three dimensions⁴⁹, studying a total of five different numerical models.

We use a continuous size polydispersity, where the particle diameter σ of each particle is randomly drawn from the following particle size distribution: $f(\sigma) = A\sigma^{-3}$, for $\sigma \in [\sigma_{\min}, \sigma_{\max}]$, where A is a normalization constant. We define the size polydispersity as $\delta = \sqrt{\overline{\sigma^2} - \bar{\sigma}^2} / \bar{\sigma}$, where $\overline{\sigma^2} = \int d\sigma f(\sigma) \sigma^2$. We mainly use $\delta = 0.23$, choosing $\sigma_{\min}/\sigma_{\max} = 0.4492$ when studying different pair potentials, as shown in Fig. 1. To investigate the effect of δ we also study the case $\delta = 0.176$ choosing $\sigma_{\min}/\sigma_{\max} = 0.543$ for the hard sphere potential. We use $\bar{\sigma}$ as the unit length. We simulate systems composed of N particles in a cubic cell of volume V with periodic boundary conditions⁴⁹. The canonical ensemble is used throughout this paper.

We use the following pairwise potential for the soft sphere models,

$$v_{ij}(r) = v_0 \left(\frac{\sigma_{ij}}{r} \right)^n + c_0 + c_1 \left(\frac{\sigma_{ij}}{r} \right)^2 + c_2 \left(\frac{\sigma_{ij}}{r} \right)^4, \quad (19)$$

$$\sigma_{ij} = \frac{(\sigma_i + \sigma_j)}{2} (1 - \eta |\sigma_i - \sigma_j|), \quad (20)$$

where v_0 is the unit of energy, and η quantifies the degree of non-additivity of the particle diameters. Non-additivity is introduced for convenience, as it prevents

more efficiently crystallization and thus it enhances glass-forming ability of the numerical models. The constants, c_0 , c_1 and c_2 , are chosen so that the first and second derivatives of $v_{ij}(r)$ become zero at the cut-off $r_{\text{cut}} = 1.25\sigma_{ij}$. We employ the additive and non-additive soft sphere models using the parameters $n = 18$, $\eta = 0$ (additive) and $n = 12$, $\eta = 0.2$ (non-additive), respectively. We set the number density $\rho = N/V = 1.0$ with $N = 1500$ for the soft sphere models.

We also use hard sphere models in three dimensions, where the pair interaction is zero for non-overlapping particles, and infinite otherwise. We employ both additive ($\eta = 0$) and non-additive ($\eta = 0.2$) systems of hard spheres, using Eq. (20). Also, we analyze an additive hard sphere system with $\delta = 0.176$. We use $N = 1000$ for the additive hard sphere systems and $N = 300$ for the non-additive systems. We have also performed simulations using $N = 300$ and 8000 for additive hard spheres with $\delta = 0.23$ and find that there is no significant finite size effects in our results. The hard sphere simulations are presented as a function of the reduced pressure $Z = P/(\rho k_B T)$, where P is the measured pressure, and $k_B T$ is set to unity.

The initial equilibrium configurations for the protocols described in Sec. III A need to be deeply supercooled either at very low temperatures (for soft sphere potentials) or high pressures (for hard spheres). To this end, we employ a swap Monte-Carlo (MC) method for all models. This approach is a very efficient thermalization algorithm which enables us to easily reach sufficiently supercooled equilibrium regimes. The details of these efficient simulations are provided in Ref. 50 for the soft sphere models and Ref. 51 for the hard sphere models.

Finally to perform the quench of the system into its inherent structure, we use a conjugate gradient method⁵² for the soft sphere systems. To realize the quench for the hard sphere systems, we perform non-equilibrium compressions up to the jamming volume fraction ϕ_J ^{53–55}. Specifically we employ the jamming algorithm described in Ref. 56 and 57 to perform these nonequilibrium compressions.

IV. NUMERICAL VALIDATION OF THE METHOD

A. Practical determination of M^*

We now present our numerical results. In Fig. 3, we show the evolution of the inherent structure energy e_{IS} (or the volume at jamming $1/\phi_J$ for hard spheres), of the overlap Q_M , and of the mean-squared displacement Δ_M as a function of M for both a soft sphere model and a hard sphere model. All the other models we have studied behave similarly. To compute Q_M , we set $a = 0.23$ for all systems. This value was used earlier to characterize metastable states and the phase transitions among them^{39,58}.

The results of the additive soft sphere model with

$\delta = 0.23$ are presented in the left panels of Fig. 3. At large M , we observe nearly constant values of $e_{\text{IS}}(M) \simeq e_{\text{IS}}(M \rightarrow \infty)$, $Q_M \simeq 1$, and $\Delta_M \simeq \Delta_\infty$, which means that the swap of the diameters within each M species marginally affects the system. Thus, after the diameter swaps, the system essentially remains in the original basin. However, with decreasing M , all observables start to deviate significantly from their large- M limits. As M decreases, we find that e_{IS} increases, $Q_M \rightarrow 0$, and Δ_M increases rapidly. These observations indicate that at smaller M , the effect of the swap is so strong that the original basin is destroyed, and the system moves to another basin.

It is clear from these figures that a clear crossover occurs between large and small M behaviors, which we wish to use to determine M^* quantitatively. However, because M^* describes a smooth crossover, it cannot be defined unambiguously. From a careful analysis of all these observables for all models, we conclude that Δ_M is the best quantity to determine M^* , because it appears as the most sensitive measure of the change of basin. As shown in Fig. 3(e), we determine M^* as the intersection of two power law regimes obeyed at large and small values. For the soft sphere model in Fig. 3(e), we obtain $M^* \simeq 8.5 - 10$ with a weak temperature dependence. These values of M^* are also reported in the figures for e_{IS} and Q_M by the vertical dashed lines. It is clear that they identify also very well the crossover behavior observed in these two observables, even though their crossover behavior is less sharply defined.

In the right panels of Fig. 3, we show the results for the additive hard sphere system with $\delta = 0.23$. We observe a behavior which is qualitatively similar to the soft sphere model, and we determine that $M^* \simeq 9 - 10$ using again the M -dependence of Δ_M in Fig. 3(f).

In addition, for hard spheres we can also compare these results obtained with the “swap and quench” protocol, to the “coarse graining and quench” protocol. The results for the latter procedure are shown with open symbols in Fig. 3. The excellent agreement between the two sets of results is evident and this second protocol thus yields the same values of M^* .

B. Results for M^* and S_{mix}^*

We have repeated the measurements shown in Fig. 3 for the five different numerical models considered in this work. For each model, we obtain M^* for a broad range of deeply supercooled state points. Finally, using the simple procedure shown in Fig. 1(b), we convert these M^* -values into an estimate of the effective mixing entropy S_{mix}^* , which we could then use to determine the configurational entropy of these continuously polydisperse systems.

We compile all our results for M^* and S_{mix}^* as a function of $1/T$ (for soft potentials) and Z (for hard spheres) in Fig. 4. The temperature and pressure scales are normalized by the mode-coupling transition points, T_c and

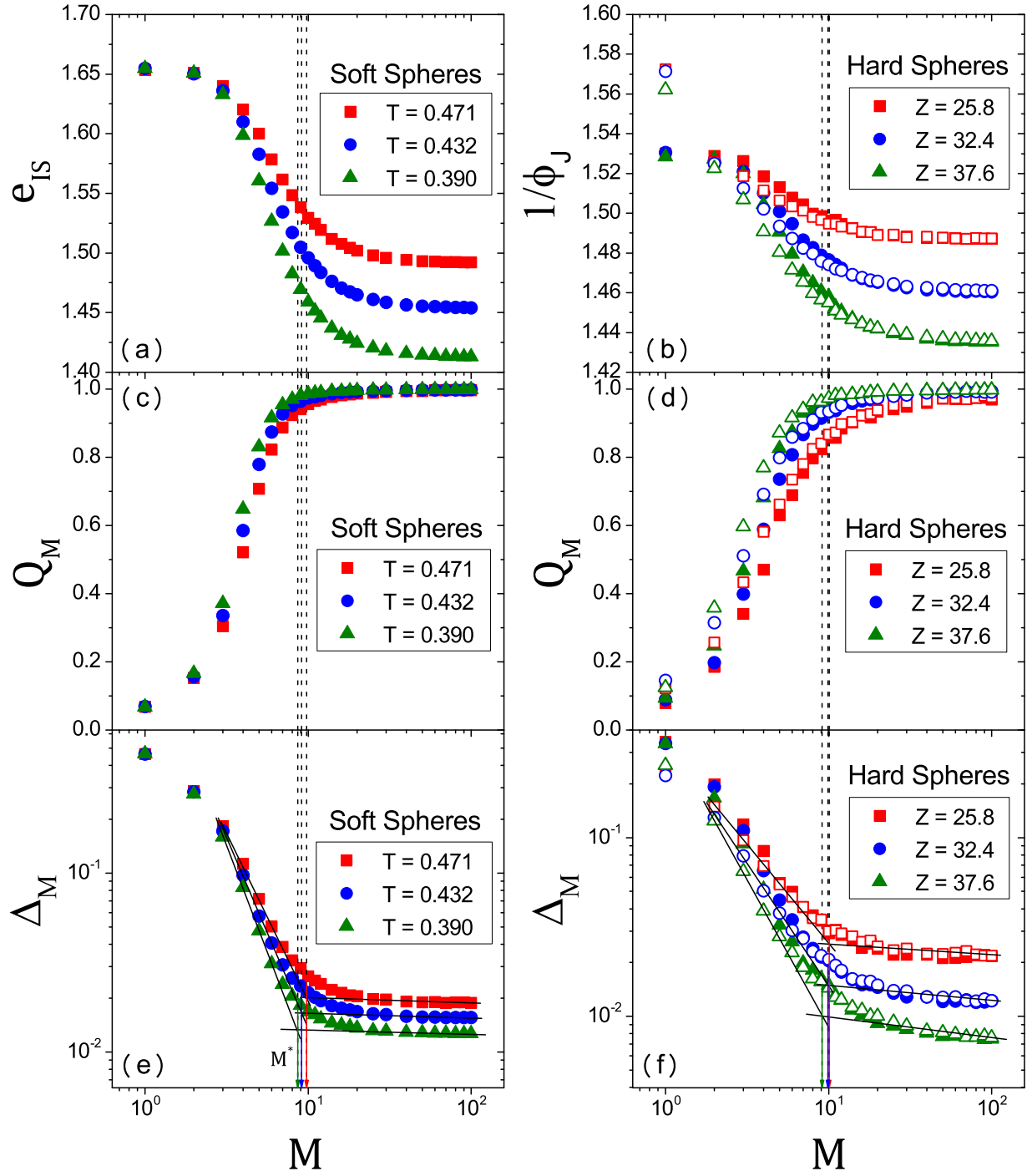


FIG. 3. (a, b) Inherent structure energy e_{IS} and volume $1/\phi_J$. (c, d) Overlap Q_M . (e, f) Mean-squared displacements Δ_M . The results are for additive soft spheres (left panels) and additive hard spheres (right panels) with $\delta = 0.23$. The vertical dashed lines represents the M^* values determined by the intersection of the two power law regimes in the mean-squared displacements in (e, f). In addition to the “swap and quench” protocol with closed symbols, results for the “coarse-graining and quench” protocol are also shown for hard spheres using open symbols.

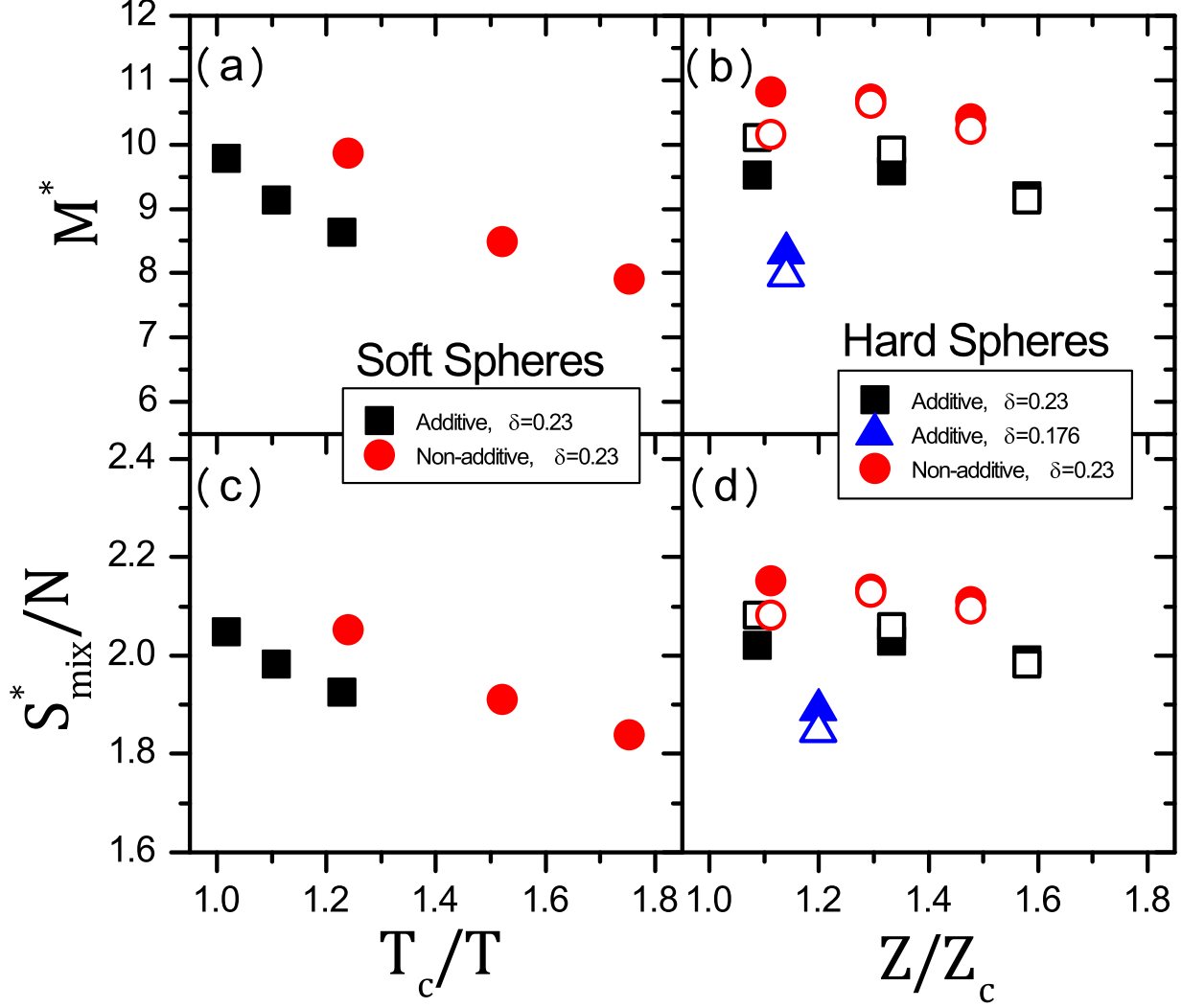


FIG. 4. Evolution of M^* for two soft sphere systems (a) and three hard sphere systems (b). (c, d) show the corresponding effective mixing entropy S_{mix}^* . The horizontal axes are normalized by the mode-coupling transition points, T_c and Z_c to facilitate the comparison between the different models. In addition to the “swap and quench” protocol (closed symbols), results for the “coarse-graining and quench” protocol (open symbols) are also shown for hard spheres.

Z_c , in order to facilitate the comparison between different glass-formers. As usual, T_c and Z_c are determined by a power-law fit of the relaxation times^{50,51}. Notice that all studied state points correspond to fluid states thermalized well beyond the mode-coupling crossover.

We find that M^* and hence S_{mix}^* slightly decrease with decreasing T or increasing Z , and this effect seems more pronounced for the soft sphere models. Physically, this reflects the fact that the basin becomes more robust against particle exchanges at lower T or higher Z . This variation is a direct confirmation that M^* represents a non-trivial characterization of the glassy states, which needs to be numerically determined independently for each state point, at least in principle.

In practice however, it is a very good approximation to consider that the effective mixing entropy S_{mix}^* of hard

spheres is essentially constant in the deeply supercooled fluid. In addition, in the hard sphere systems the two distinct protocols introduced above give quantitatively consistent values, especially at large Z , which again confirms the robustness of our numerical approach.

Remarkably, the value of M^* for the additive system with $\delta = 0.176$ is about 20% smaller than that of the system with $\delta = 0.23$, which may be rationalized by the corresponding relative reduction of the polydispersity (of about $\approx 23\%$). Thus, our results appear in agreement with the physical expectation that $(M^* - 1)$ should be proportional to the polydispersity δ . We would need more data at different polydispersities to confirm this result quantitatively. However, a rough extrapolation of these M^* values towards smaller polydispersity values, suggests that $M^* \simeq 4 - 5$ for $\delta = 0.10$ and

$M^* \simeq 2 - 3$ for $\delta \simeq 0.05$, whereas smaller polydisperse systems should essentially be treated as mono-component systems. We can also translate these findings into a critical value $(1 + \epsilon^*) \simeq 1.1$ for the size ratio below which two particles should be treated as having the same size.

Finally, we note that for the relatively polydisperse systems that we study, the effective mixing entropies are of order $S_{\text{mix}}^*/N \simeq 2.0$. Given that the configurational entropy is typically of order $S_{\text{conf}}/N \simeq 1.0$ near the onset of slow dynamics^{18,20}, we conclude that an accurate determination of the mixing entropy is indeed crucial to properly estimate the configurational entropy.

V. DISCUSSION AND PERSPECTIVES

In this paper, we discussed the problems of the conceptual definition and of the practical measurement of the configurational entropy S_{conf} in glass-forming models characterized by a polydisperse size distribution, inspired by the physics of colloidal materials. We first noticed that standard approaches to estimate the configurational entropy fail in the case of a continuous polydispersity, providing either an infinite or an incorrect estimate of S_{conf} depending on an arbitrary choice made regarding the mixing entropy contribution. We then proposed a simple method to compute a finite and physically-meaningful configurational entropy S_{conf} in continuously polydisperse systems which relies on a treatment of the original system as an effective M^* -component system, where M^* is finite and has to be measured directly at each state point. Finally, we performed numerical simulations of five different glass-forming models and showed that our approach provides meaningful results in all cases.

The key idea leading to a finite configurational entropy for polydisperse systems is the distinction between *configurations* (or their corresponding inherent structures) in the phase space volume and *states* defined as free energy minima. While the configurational entropy should be interpreted or quantified as the (logarithm of the) number of states, the inherent structure approaches instead quantify the (logarithm of the) number of inherent structures associated to configurations. While this may represent a correct approximation in some specific instances, the confusion between the two concepts has important consequences for polydisperse mixtures, as the number of configurations (and hence of inherent structures) diverges, while the number of states does not. This conceptual distinction has been discussed at length in the literature^{14,59}, as the confusion between states and configurations is at the root of several arguments suggesting the impossibility of an ideal glass transition⁶⁰⁻⁶². Therefore, the case of polydisperse materials is one more instance where this confusion may lead to paradoxical results.

We mentioned in the introduction the recently-proposed alternative method to compute the configurational entropy, based on the Franz-Parisi construction, which relies on estimating the free energy difference be-

tween the fluid and glass states^{31,38}. This method does not suffer from a possible divergence in the mixing entropy, because it does not involve estimating the entropy of the fluid and glass states separately.

In fact, the conceptual difference between the standard approach ($S_{\text{conf}} = S_{\text{tot}} - S_{\text{vib}}$) and the Franz-Parisi construction is easy to grasp from their practical implementations. Both approaches rely on performing thermodynamic measurements on systems constrained to evolve ‘near’ a given reference configuration. When using the Frenkel-Ladd method in the standard approach^{17,19,20}, the constraint is a set of harmonic springs connecting *each particle* to reside close to its position in the reference configuration. Instead, in the Franz-Parisi approach, one constrains the *collective density profile* to reside close to the one of the reference configuration. For the particular case of polydisperse systems, the collective nature of this constraint allows particle permutations in the glass state which are then automatically taken into account with their correct equilibrium weight. In order to use the standard approach we have shown that it is necessary to correct for the (incorrect) ‘self’ nature of the constraint by estimating separately an effective mixing entropy contribution, and we have proposed a simple method to do so.

Because both methods provide distinct conceptual estimates of the configurational entropy, there is no reason why they should yield identical absolute values of S_{conf} in the supercooled liquid regime. In the presence of a genuine ideal glass transition, however, both methods should yield consistent results for its location. In Ref. 39, we have computed the volume fraction dependence of the absolute value of S_{conf} for the additive hard sphere system with $\delta = 0.23$ studied in the present work, using both the present approach and the Franz-Parisi construction. The results show that the agreement between the two methods is good³⁹.

Note that in experiment, the configurational entropy is obtained by integration of the heat capacity difference between the fluid and crystal states⁶³, where it is assumed that the vibrational (or glass) entropy is well approximated by the entropy of the crystal^{64,65}. The reference point which sets the absolute value of the configurational entropy is given by the entropy of fusion. Therefore, traditional experimental measurements of the configurational entropy do not suffer from the problem of the mixing entropy, because the experimental procedure does not require estimating the absolute entropy of any state point. Of course, the drawback of this procedure is that it is unclear whether the experimental protocol truly reflects the theoretical definition of a configurational entropy related to the number of free energy minima. Therefore, for theoretical purposes we do not wish to follow the experimental procedure to solve the issue raised by polydispersity. Similarly, the experimental path cannot be followed in computer simulations where the properties of the crystal are usually unknown.

Our numerical protocol, which transforms a continu-

ously polydisperse system into an M^* -component system, is also useful for more general theoretical investigations, since finite mixtures are theoretically more tractable than continuously polydisperse systems^{17,42,66}. For example, theoretical computations of the thermodynamics of the glass phase in (finite and discrete) multi-components mixtures^{17,42} could more easily be applied once M^* is numerically determined. In the same vein, in Ref. 66, the multi-components extension of the mode coupling theory is compared with simulations of a continuous polydisperse system with $\delta = 5.8\%$. The theory seems to describe well simulation results regarding glassy dynamical behaviors when $M \geq 3$, which is in good agreement with the estimate obtained in our work assuming that $(M^* - 1)$ is proportional to δ . Our work in fact paves the way for an analytical treatment of the glass thermodynamics of continuously polydisperse particle systems. Another interesting theoretical goal would be the analytical derivation of the critical size ratio $(1 + \epsilon^*)$ separating the regime where particles should be treated as identical or as distinct, as this would allow a fully analytical treatment of polydisperse materials. When applied to hard spheres, predictions could then be made regarding the influence of the polydispersity on the jamming transition, which is another topic of interest.

ACKNOWLEDGMENTS

We thank P. Charbonneau, D. Coslovich, A. Ikeda, H. Ikeda, A. Ninarello, G. Tarjus, and F. Zamponi for helpful comments. We specially thank A. Ninarello for providing us with very low temperature configurations for the soft sphere models. The research leading to these results has received funding from the European Research Council under the European Unions Seventh Framework Programme (FP7/2007-2013)/ERC Grant Agreement No. 306845. This work was supported by a grant from the Simons Foundation (# 454933, Ludovic Berthier)

- ¹W. Poon, "Colloids as big atoms," *Science* **304**, 830 (2004).
- ²M. E. Cates and V. N. Manoharan, "Celebrating soft matter's 10th anniversary: Testing the foundations of classical entropy: colloid experiments," *Soft Matter* **11**, 6538 (2015).
- ³J. Salacuse and G. Stell, "Polydisperse systems: statistical thermodynamics, with applications to several models including hard and permeable spheres," *J. Chem. Phys.* **77**, 3714 (1982).
- ⁴J. Briano and E. Glandt, "Statistical thermodynamics of polydisperse fluids," *J. Chem. Phys.* **80**, 3336 (1984).
- ⁵P. B. Warren, "Combinatorial entropy and the statistical mechanics of polydispersity," *Phys. Rev. Lett.* **80**, 1369 (1998).
- ⁶P. Sollich and M. E. Cates, "Projected free energies for polydisperse phase equilibria," *Phys. Rev. Lett.* **80**, 1365 (1998).
- ⁷P. Sollich, "Predicting phase equilibria in polydisperse systems," *J. Phys.: Condens. Matter* **14**, R79 (2001).
- ⁸R. H. Swendsen, "Gibbs' paradox and the definition of entropy," *Entropy* **10**, 15 (2008).
- ⁹D. Frenkel, "Why colloidal systems can be described by statistical mechanics: some not very original comments on the gibbs paradox," *Mol. Phys.* **112**, 2325 (2014).
- ¹⁰J. Zhang, R. Blaak, E. Trizac, J. A. Cuesta, and D. Frenkel, "Optimal packing of polydisperse hard-sphere fluids," *J. Chem. Phys.* **110**, 5318 (1999).
- ¹¹F. Paillusson and I. Pagonabarraga, "On the role of composition entropies in the statistical mechanics of polydisperse systems," *J. Stat. Mech.* **2014**, P10038 (2014).
- ¹²W. Kauzmann, "The nature of the glassy state and the behavior of liquids at low temperatures," *Chem. Rev.* **43**, 219 (1948).
- ¹³G. Adam and J. H. Gibbs, "On the temperature dependence of cooperative relaxation properties in glass-forming liquids," *J. Chem. Phys.* **43**, 139 (1965).
- ¹⁴L. Berthier and G. Biroli, "Theoretical perspective on the glass transition and amorphous materials," *Rev. Mod. Phys.* **83**, 587 (2011).
- ¹⁵G. Biroli and J. Kurchan, "Metastable states in glassy systems," *Phys. Rev. E* **64**, 016101 (2001).
- ¹⁶P. Charbonneau, J. Kurchan, G. Parisi, P. Urbani, and F. Zamponi, "Fractal free energy landscapes in structural glasses," *Nat. Commun.* **5** (2014).
- ¹⁷B. Coluzzi, M. Mézard, G. Parisi, and P. Verrocchio, "Thermodynamics of binary mixture glasses," *J. Chem. Phys.* **111**, 9039 (1999).
- ¹⁸F. Sciortino, W. Kob, and P. Tartaglia, "Inherent structure entropy of supercooled liquids," *Phys. Rev. Lett.* **83**, 3214 (1999).
- ¹⁹S. Sastry, "Evaluation of the configurational entropy of a model liquid from computer simulations," *J. Phys.: Condens. Matter* **12**, 6515 (2000).
- ²⁰L. Angelani and G. Foffi, "Configurational entropy of hard spheres," *J. Phys.: Condens. Matter* **19**, 256207 (2007).
- ²¹F. Sciortino, "Potential energy landscape description of supercooled liquids and glasses," *J. Stat. Mech.* **2005**, P05015 (2005).
- ²²G. L. Hunter and E. R. Weeks, "The physics of the colloidal glass transition," *Rep. Prog. Phys.* **75**, 066501 (2012).
- ²³S. Gokhale, A. Sood, and R. Ganapathy, "Deconstructing the glass transition through critical experiments on colloids," *Adv. Phys.* **65**, 363 (2016).
- ²⁴L. Santen and W. Krauth, "Absence of thermodynamic phase transition in a model glass former," *Nature* **405**, 550 (2000).
- ²⁵Y. Brumer and D. R. Reichman, "Numerical investigation of the entropy crisis in model glass formers," *J. Phys. Chem. B* **108**, 6832 (2004).
- ²⁶T. Kawasaki, T. Araki, and H. Tanaka, "Correlation between dynamic heterogeneity and medium-range order in two-dimensional glass-forming liquids," *Phys. Rev. Lett.* **99**, 215701 (2007).
- ²⁷M. Hermes and M. Dijkstra, "Thermodynamic signature of the dynamic glass transition in hard spheres," *J. Phys.: Condens. Matter* **22**, 104114 (2010).
- ²⁸E. Zaccarelli, S. M. Liddle, and W. C. Poon, "On polydispersity and the hard sphere glass transition," *Soft Matter* **11**, 324 (2015).
- ²⁹R. J. Speedy, "The entropy of a glass," *Mol. Phys.* **80**, 1105 (1993).
- ³⁰S. Sastry, "The relationship between fragility, configurational entropy and the potential energy landscape of glass-forming liquids," *Nature* **409**, 164 (2001).
- ³¹L. Berthier and D. Coslovich, "Novel approach to numerical measurements of the configurational entropy in supercooled liquids," *Proc. Natl. Acad. Sci. U. S. A.* **111**, 11668 (2014).
- ³²D. Asenjo, F. Paillusson, and D. Frenkel, "Numerical calculation of granular entropy," *Phys. Rev. Lett.* **112**, 098002 (2014).
- ³³S. Martiniani, K. J. Schrenk, J. D. Stevenson, D. J. Wales, and D. Frenkel, "Turning intractable counting into sampling: Computing the configurational entropy of three-dimensional jammed packings," *Phys. Rev. E* **93**, 012906 (2016).
- ³⁴R. Vink and G. Barkema, "Configurational entropy of network-forming materials," *Phys. Rev. Lett.* **89**, 076405 (2002).
- ³⁵A. Anikeenko, N. Medvedev, and T. Aste, "Structural and entropic insights into the nature of the random-close-packing limit," *Phys. Rev. E* **77**, 031101 (2008).
- ³⁶Y. Zhou and S. T. Milner, "Structural entropy of glassy systems from graph isomorphism," *Soft Matter* (2016).

- ³⁷P. Ronceray and P. Harrowell, “From liquid structure to configurational entropy: introducing structural covariance,” *J. Stat. Mech.* **2016**, 084002 (2016).
- ³⁸S. Franz and G. Parisi, “Phase diagram of coupled glassy systems: A mean-field study,” *Phys. Rev. Lett.* **79**, 2486 (1997).
- ³⁹L. Berthier, P. Charbonneau, D. Coslovich, A. Ninarello, M. Ozawa, and S. Yaida, “(in preparation),” (2016).
- ⁴⁰R. J. Speedy, “The hard sphere glass transition,” *Mol. Phys.* **95**, 169 (1998).
- ⁴¹M. Ozawa, W. Kob, A. Ikeda, and K. Miyazaki, “Equilibrium phase diagram of a randomly pinned glass-former,” *Proc. Natl. Acad. Sci. U. S. A.* **112**, 6914 (2015).
- ⁴²I. Biazio, F. Caltagirone, G. Parisi, and F. Zamponi, “Theory of amorphous packings of binary mixtures of hard spheres,” *Phys. Rev. Lett.* **102**, 195701 (2009).
- ⁴³W. Kob and H. C. Andersen, “Testing mode-coupling theory for a supercooled binary lennard-jones mixture i: The van hove correlation function,” *Phys. Rev. E* **51**, 4626 (1995).
- ⁴⁴D. Frenkel and A. J. Ladd, “New monte carlo method to compute the free energy of arbitrary solids. application to the fcc and hcp phases of hard spheres,” *J. Chem. Phys.* **81**, 3188 (1984).
- ⁴⁵V. Ogarko and S. Luding, “Equation of state and jamming density for equivalent bi-and polydisperse, smooth, hard sphere systems,” *J. Chem. Phys.* **136**, 124508 (2012).
- ⁴⁶V. Ogarko and S. Luding, “Prediction of polydisperse hard-sphere mixture behavior using tridisperse systems,” *Soft Matter* **9**, 9530 (2013).
- ⁴⁷F. H. Stillinger and T. A. Weber, “Hidden structure in liquids,” *Phys. Rev. A* **25**, 978 (1982).
- ⁴⁸F. H. Stillinger, “Exponential multiplicity of inherent structures,” *Phys. Rev. E* **59**, 48 (1999).
- ⁴⁹M. P. Allen and D. J. Tildesley, *Computer simulation of liquids* (Oxford University Press, 1989).
- ⁵⁰A. Ninarello, L. Berthier, and D. Coslovich, “(in preparation),” (2016).
- ⁵¹L. Berthier, D. Coslovich, A. Ninarello, and M. Ozawa, “Equilibrium sampling of hard spheres up to the jamming density and beyond,” *Phys. Rev. Lett.* **116**, 238002 (2016).
- ⁵²J. Nocedal and S. Wright, *Numerical optimization* (Springer Science & Business Media, 2006).
- ⁵³F. H. Stillinger and T. A. Weber, “Inherent structure theory of liquids in the hard-sphere limit,” *J. Chem. Phys.* **83**, 4767 (1985).
- ⁵⁴P. Chaudhuri, L. Berthier, and S. Sastry, “Jamming transitions in amorphous packings of frictionless spheres occur over a continuous range of volume fractions,” *Phys. Rev. Lett.* **104**, 165701 (2010).
- ⁵⁵M. Ozawa, T. Kuroiwa, A. Ikeda, and K. Miyazaki, “Jamming transition and inherent structures of hard spheres and disks,” *Phys. Rev. Lett.* **109**, 205701 (2012).
- ⁵⁶N. Xu, J. Blawdziewicz, and C. S. O’Hern, “Random close packing revisited: Ways to pack frictionless disks,” *Phys. Rev. E* **71**, 061306 (2005).
- ⁵⁷K. W. Desmond and E. R. Weeks, “Random close packing of disks and spheres in confined geometries,” *Phys. Rev. E* **80**, 051305 (2009).
- ⁵⁸L. Berthier and R. L. Jack, “Evidence for a disordered critical point in a glass-forming liquid,” *Phys. Ref. Lett.* **114**, 205701 (2015).
- ⁵⁹G. Biroli and R. Monasson, “From inherent structures to pure states: Some simple remarks and examples,” *EPL* **50**, 155 (2000).
- ⁶⁰F. H. Stillinger, “Supercooled liquids, glass transitions, and the kauzmann paradox,” *J. Chem. Phys.* **88**, 7818 (1988).
- ⁶¹A. Donev, F. H. Stillinger, and S. Torquato, “Configurational entropy of binary hard-disk glasses: Nonexistence of an ideal glass transition,” *J. Chem. Phys.* **127**, 124509 (2007).
- ⁶²J.-P. Eckmann and I. Procaccia, “Ergodicity and slowing down in glass-forming systems with soft potentials: No finite-temperature singularities,” *Phys. Rev. E* **78**, 011503 (2008).
- ⁶³R. Richert and C. Angell, “Dynamics of glass-forming liquids. v. on the link between molecular dynamics and configurational entropy,” *J. Chem. Phys.* **108**, 9016 (1998).
- ⁶⁴O. Yamamuro, I. Tsukushi, A. Lindqvist, S. Takahara, M. Ishikawa, and T. Matsuo, “Calorimetric study of glassy and liquid toluene and ethylbenzene: Thermodynamic approach to spatial heterogeneity in glass-forming molecular liquids,” *J. Phys. Chem. B* **102**, 1605 (1998).
- ⁶⁵C. Angell and S. Borick, “Specific heats c_p , c_v , c_{conf} and energy landscapes of glassforming liquids,” *J. Non-Cryst. Solids* **307**, 393 (2002).
- ⁶⁶F. Weysser, A. M. Puertas, M. Fuchs, and T. Voigtman, “Structural relaxation of polydisperse hard spheres: Comparison of the mode-coupling theory to a langevin dynamics simulation,” *Phys. Rev. E* **82**, 011504 (2010).